Research Article | Vol. 29, No. 3 / 1 February 2021 / Optics Express 3873
Optics EXPRESS

Detection of aflatoxin M1 by fiber cavity attenuated phase shift spectroscopy

M. Daniyal Ghauri,[1] Syed Zajif Hussain,[2] Ubaid Ullah,[1] Rana M. Armaghan Ayaz,[3] Rahman Shah Zaib Saleem,[2] Alper Kiraz,[3] and M. Imran Cheema[1,*]

[1]Department of Electrical Engineering, Syed Babar Ali School of Science and Engineering, Lahore University of Management Sciences, Lahore 54792, Pakistan
[2]Department of Chemistry and Chemical Engineering, Syed Babar Ali School of Science and Engineering, Lahore University of Management Sciences, Lahore 54792, Pakistan
[3]Department of Physics, Koç University, 34450 Sariyer, Istanbul, Turkey
*imran.cheema@lums.edu.pk

Abstract: Aflatoxin M1 (AFM1) is a carcinogenic compound commonly found in milk in excess of the WHO permissible limit, especially in developing countries. Currently, state-of-the-art tests for detecting AFM1 in milk include chromatographic systems and enzyme-linked-immunosorbent assays. Although these tests provide fair accuracy and sensitivity, they require trained laboratory personnel, expensive infrastructure, and many hours to produce final results. Optical sensors leveraging spectroscopy have a tremendous potential of providing an accurate, real-time, and specialist-free AFM1 detector. Despite this, AFM1 sensing demonstrations using optical spectroscopy are still immature. Here, we demonstrate an optical sensor that employs the principle of cavity attenuated phase shift spectroscopy in optical fiber cavities for rapid AFM1 detection in aqueous solutions at 1550 nm. The sensor constitutes a cavity built by two fiber Bragg gratings. We splice a tapered fiber of < 10 μm waist inside the cavity as a sensing head. For ensuring specific binding of AFM1 in a solution, the tapered fiber is functionalized with DNA aptamers followed by validation of the conjugation via FTIR, TGA, and EDX analyses. We then detect AFM1 in a solution by measuring the phase shift between a sinusoidally modulated laser input and the sensor output at resonant frequencies of the cavity. Our results show that the sensor has the detection limit of 20 ng/L (20 ppt), which is well below both the U.S. and the European safety regulations. We anticipate that the present work will lead towards a rapid and accurate AFM1 sensor, especially for low-resource settings.

© 2021 Optical Society of America under the terms of the OSA Open Access Publishing Agreement

1. Introduction

The feed of animals is often contaminated by a specific fungus, resulting in contamination of the produced milk with aflatoxin M1 [1]. Aflatoxin M1 (AFM1) is a carcinogenic compound, which, if exceeded to a certain level, can cause serious health concerns to people [2]. Given the hazardous nature of the contamination, many countries have established guidelines for maximum permissible levels of AFM1 in milk. For example, the United States and European regulatory bodies limit the amount of AFM1 to 500 ng/L and 50 ng/L, respectively [1].

Currently, well-established methods of effective detection of AFM1 include thin-layer chromatography, high performance liquid chromatography, and immunoassays such as enzyme-linked immunosorbent assay [3]. The frequent adaptation of these techniques, especially in the developing countries, is usually hindered due to the need for significant maintenance and operator expertise, extensive sample pre-treatments, time-consuming analyses, and high infrastructure costs. A variety of optical sensors based upon surface plasmon resonance (SPR), interferometry, cavities, and fluorescence can overcome previously mentioned limitations. However, so far in the literature, very few optical sensors have been reported for AFM1 detection.

#408975 https://doi.org/10.1364/OE.408975
Journal © 2021 Received 1 Sep 2020; revised 11 Nov 2020; accepted 15 Jan 2021; published 25 Jan 2021

Optics EXPRESS

In one of the promising approaches, researchers utilized long range SPR in conjunction with fluorophore-labeled AFM1 molecules for demonstrating a highly sensitive and rapid sensor [4]. In another compact fluorometric system, researchers provided preliminary screening of milk for AFM1 by using LED, detector, and associated optics [5]. However, all the fluorescence-based techniques involve an arduous labeling process, and the fluorophores' locations cannot be accurately controlled. This introduces uncertainty in the detected signal and creates significant challenges to produce repeatable and accurate results [6,7]. Moreover, apart from sensors based upon optical cavities, all others are generally single pass, i.e., an optical wave interacts with a sample only once. Whereas in a cavity-based sensor, optical waves sample an analyte numerous times, and thus highly accurate, sensitive, and rapid detection scheme can be realized. Motivated by this, researchers demonstrated a sensor based on silicon oxynitride ring resonators for AFM1 detection [8]. They demonstrated 4.1 μg/L AFM1 detection in a DMSO solution. Their technique was based upon the frequency domain, i.e., they looked at the shift in a cavity resonant peak as a function of an AFM1 binding event. The frequency domain approach offers low noise immunity compared to the time domain approach in optical cavities [9]. The development of ring resonator based sensing platforms also has challenges in accurately fabricating the ring and coupling waveguide with a precise gap. To overcome these drawbacks, recently, researchers demonstrated an Si_3N_4 asymmetric Mach-Zehnder interferometer (aMZI) for AFM1 detection [10]. Although the aMZI sensor has the required limit of detection, however, fabricating such a device is extremely challenging in low-resource settings where microfabrication facilities are generally not available. Motivated from this, we demonstrate an optical sensor for AFM1 detection that not only has the desired limit of detection but may also be easily developed and used in low-resource settings.

Herbelin et al. first developed cavity attenuated phase shift spectroscopy (CAPS) in the early 1980s to determine mirrors' reflectivity in free space cavities [11,12]. In CAPS, light from a CW laser source is amplitude modulated with angular frequency ω_m and is injected into a cavity. With respect to the input light, the output light from the cavity has a phase shift, ϕ, that is related to the ring down time, τ, of the cavity as

$$\tan\phi = -\omega_m\tau, \tag{1}$$

where the minus sign indicates that the cavity output lags the input. The constant monitoring of ϕ then gives continuous information about τ and consequently, information about any attenuation events inside the cavity. CAPS and one of its well-established variants, cavity ring down spectroscopy (CRDS), have been successfully applied in the gaseous phase for various applications using free space cavities [13–15].

For liquid phase applications, free space cavities pose a variety of challenges, including instability of the cavity and the degradation of mirrors due to liquid inside the cavity [16,17]. These challenges have been overcome by utilizing microcavities [9,18] and fiber-based cavities and loops [19] for various liquid phase applications. Recently researchers applied CRDS in fiber loops for detecting aflatoxin B1 in a solution [20]. They did not apply any surface functionalization protocol to the sensing head and demonstrated the 16 μg/L detection limit.

CAPS and its variants have never been utilized to detect AFM1 either in free space or fiber-based structures. Moreover, in all laser-based fiber platforms utilizing CAPS, generally, the Pound-Drever-Hall (PDH) technique is required for parking the laser for continuous monitoring of the phase shift. Here, we demonstrate an optical fiber sensor that not only utilizes the principle of CAPS for the first time to detect AFM1 but also involves a more straightforward experimental setup that does not require the use of the PDH technique. We show that our sensor has the detection limit of 20 ng/L (20 ppt), which is lower than the limits imposed by US and European authorities.

Optics EXPRESS

The paper's organization is such that Section 2. gives detailed experimental procedures that include surface functionalization protocol and the sensor architecture. It is followed by Section 3., which discusses the results of the demonstrated sensor. Finally, Section 4. concludes the paper along with some suggestions for future work.

2. Experimental procedures

In this section, we discuss various steps involved in developing the AFM1 sensor.

2.1. Sensing head and its surface functionalization

For developing the sensing head, we taper an optical fiber to expose its core for the interaction of the optical wave with an analyte. The tapered fiber is fabricated by pulling an SMF-28 fiber with computer-controlled motorized stages while simultaneously heating the fiber with a butane flame. We fix the fabricated tapered fiber on a U-shaped piece of a copper-clad printed circuit board (PCB) using the nichrome soldering and then safely remove it from the tapering setup. The use of alloy to fix the tapered fiber is critical as generally glues or epoxies malfunction with the application of abrasive chemicals like piranha during the functionalization steps. We adapt the surface functionalization protocol reported in Ref. [21] for our sensing head. The Ref. [21] uses DNA aptamers for functionalizing SiN microring resonators, whereas we report the application of aptamers for conjugating silica tapered fibers.

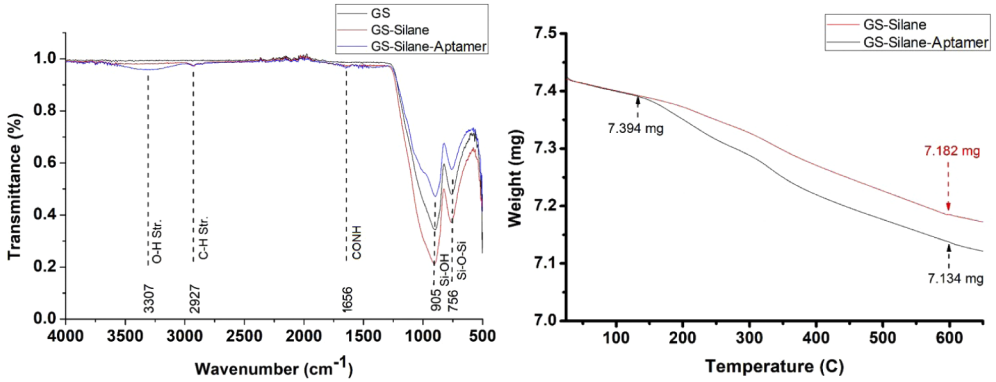
In the present work, we first anneal the U-shaped copper PCB containing the silica tapered optical fiber at 1050°C for 1.5 hours for removing any organic contaminants from the tapered fiber. For hydroxylation, we orient the U-shaped PCB in such a way that the fiber is dipped into a curved petri dish containing the piranha solution. We then repeat the same procedure for silanization of the fiber with 0.01%, V/V solution of 3-glycidoxypropyl methyldiethoxy silane prepared in anhydrous-toluene. The petri dish is then heated at 60°C for 10 min. The fiber is then immersed into 100 μM solution of a DNA aptamer having one end terminated with the amino group, 5AmMC6 /GTTGGGCACGTGTTGTCTCTCTGTGTCTCGTGCCCTTCGCTAGGCCCACA, maintained in a phosphate buffer having a pH of 8. All chemicals used in the functionalization process are purchased from Sigma Aldritch Inc. USA except the aptamer, which is obtained from IDT integrated DNA technologies Inc. USA.

The protocol's initial implementation is done on a glass slide since its surface properties are very similar to a silica fiber. The FTIR results presented in Fig. 1(a) show that the silanization followed by the conjugation of DNA aptamers are successfully achieved on the glass substrate. The characteristic peaks appearing in the substrate's FTIR spectrum at 756 and 905 cm^{-1} correspond respectively to its Si-OH and Si-O-Si functionalities. After the silanization process, the intensities of these peaks rise, indicating an increase in the number of these functionalities over the substrate surface. In addition to this, the peaks appearing between 2840 and 3000 cm^{-1} also narrate the presence of C-H bonds signaling the successful silanization. Besides this, the conjugation of DNA aptamer on the silanized glass slide is verified by the suppression of peaks at 756 and 905 cm^{-1}, and the respective appearance of O-H stretching and amide bands at 3307 and 1656 cm^{-1}.

In the second phase, the protocol is implemented on a non-tapered SMF-28 fiber. The thermogravimetric analysis (TGA) for the processed fiber in Fig. 1(b) indicates that the developed surface chemistry protocol is working on the fiber. This is confirmed by noting the loss of weight in the fiber conjugated with the DNA aptamer compared to the silanized fiber. The weight reduction is due to the burning of organic contents added by the DNA aptamer.

The protocol is implemented on tapered fibers in the third phase of the surface functionalization. Here, we utilize the energy-dispersive X-ray spectroscopy (EDX) for comparing the elemental compositions of non-functionalized and functionalized tapered optical fibers, as shown Fig. 2. The presence of extra signals of carbon and nitrogen elements in the EDX mapping of the

Optics EXPRESS



(a) (b)

Fig. 1. (a) FTIR results showing silanization and conjugation of DNA apatmers over the surface of a glass substrate (GS). (b) Thermogravimetric analysis presenting weight loss of silanes and silanes + DNA-Aptamer conjugated separately over the surface of an SMF-28 optical fiber

functionalized tapered fiber compared to the non-functionalized one confirms a successful conjugation process.

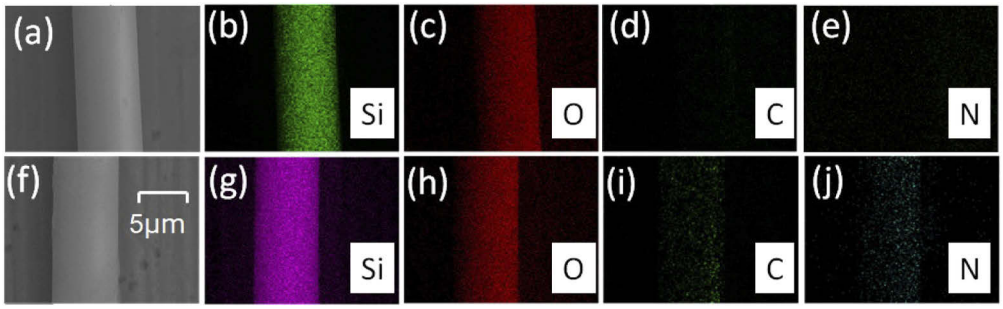


Fig. 2. (a-e) and (f-j) are EDX mapping analysis of the non-functionalized and functionalized tapered fibers, respectively. The presence of silicon (Si) and oxygen (O) shows silica fibers in both of the cases. Carbon (C) and nitrogen (N) are present only in the functionalized fiber due to silanes and DNA aptamers. The scale is 5μm for all images.

2.2. Experimental setup

The schematics of our sensor for conducting CAPS measurements with fiber cavities are shown in Fig. 3. We first build an optical fiber cavity by using fiber Bragg gratings (FBGs) at the two ends of SMF-28 fiber. The two FBGs are purchased from Oeland Inc. Canada with parameters of FBG_1: 1549.99 nm, 91.49%, 0.28 nm and FBG_2: 1550.02 nm, 99.44%, 0.23 nm. The first, second, and third parameters refer to the central wavelength, reflectivity, and full width half max bandwidth, respectively. The functionalized tapered fiber (waist diameter $\approx$ 8.5 μm) is then spliced between the two FGBs, which results in the overall cavity length of 32 cm. We then package the U-shaped piece containing the tapered fiber portion into a 3D-printed fluidic cell to deliver a sample to the tapered portion efficiently.

The sensor source is a 1550 nm continuous wave laser diode purchased from Eblana Photonics (EP1550-0-NLW-B26-100FM) and operated with Thorlabs CLD1015 controller. For initiating

Optics EXPRESS

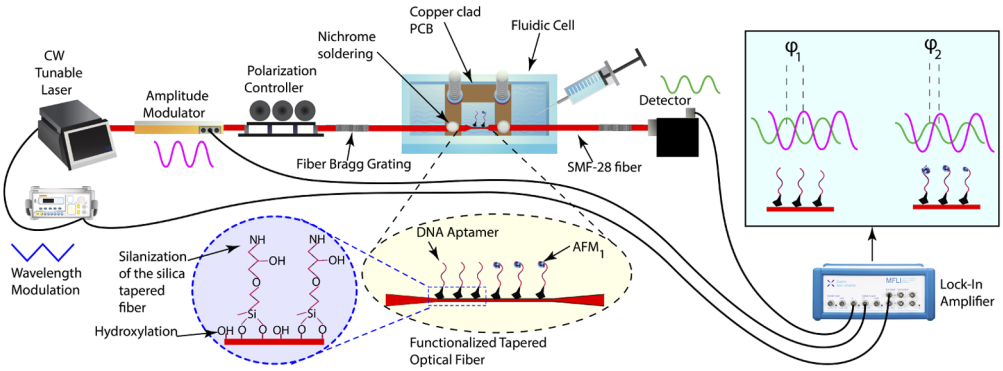


Fig. 3. Schematics (not drawn to scale) for the sensor for detecting AFM1 using the cavity attenuated phase spectroscopy (CAPS). The phase shifts and modulations depths are exaggerated for illustrating the CAPS measurement where $|\phi_1|>|\phi_2|$. Note that the tapered fiber is straight and only its holder is U-shaped.

the CAPS measurements, we sinusoidally modulate (4 MHz, 1 V_{pp}) the laser using an external Mach-Zehnder modulator (Sumitomo Osaka T.MZH1.5-10PD-ADC). For scanning the cavity resonances, the laser is current tuned continuously using a triangular wave (5 mHz, 100 mVpp). The simultaneous current and amplitude modulations allow us to conduct CAPS measurements at resonant peaks without needing the PDH technique [9]. The laser wavelength is tuned slow enough to allow a proper build-up of the cavity for conducting stable measurements. The modulated laser output is injected into the cavity, and the same signal is used as a reference input signal to the lock-in amplifier (Zurich Instruments MFLI). An InGaAs photodetector (Thorlabs DET08CFC/M) is used for monitoring the cavity output which in turn is connected to the signal port of the lock-in amplifier.

In traditional CAPS systems, one is required to use a source wavelength that matches the maximum absorption wavelength of an analyte to be probed. In our case, we are not restricted to using the absorption wavelength of the AFM1 as losses are mainly introduced due to the tapered fiber's evanescent field, as explained below.

The phase change principle is based on cavity attenuated phase shift spectroscopy (CAPS), i.e., it is mainly governed by Eq. (1.). The ring down time, τ, and hence phase, ϕ, changes whenever the losses in the cavity changes. In our sensing setup, the tapered fiber acts as a sensing head. The tapered fiber causes the propagating optical mode in the cavity to probe the surroundings around it evanescently. The tapered fiber is functionalized with DNA aptamers to increase the specificity and sensitivity of AFM1 in a solution. Once AFM1 binds with DNA aptamers on the tapered fiber, the optical mode experiences loss, and hence the overall attenuation in the cavity increases. This process decreases the ring down, and hence the phase decreases. One can also think that as AFM1 binding events occur, the refractive index of surroundings around the tapered fiber increases. This, in turn, pushes the optical mode out of the cavity, and hence overall losses increase in the cavity.

3. Results

A representative CAPS measurement for an FBG based cavity is shown in Fig. 4. We observe that, in comparison to the position of a resonance peak, the absolute phase maximum is red-shifted and blue-shifted during the decreasing and increasing wavelength scans, respectively. This behavior can be explained by solving coupled mode equations for a transmission cavity [22] with a sinusoidally modulated laser input [23]. We obtain the following solutions for the magnitude

Optics EXPRESS

and phase of the output cavity field

$$|E_{op}| = \frac{c\tau\sqrt{(1-R_1)(1-R_2)}}{2nl\sqrt{1+\tau^2(\omega-\omega_o+\omega_m)^2}}|E_{in}|, \tag{2}$$

$$\tan\phi = -(\omega-\omega_o+\omega_m)\tau, \tag{3}$$

where, R_1 and R_2 are reflectivities of the two FBGs, c is the speed of light, n is the SMF-28 fiber effective index, l is the cavity length, ω_o is a resonant frequency of the cavity, and ω is the laser scan frequency. At a resonant frequency, $\omega = \omega_o$, Eqs. (2) and (3) reduce to the classical CAPS equations. It is evident from Eq. (2) that $|E_{op}|$ is always maximum whenever $\omega = \omega_o - \omega_m \approx \omega_o$. In the case of Eq. (3), it is clear that $|\tan\phi|$ is maximum whenever $\omega > (\omega_o - \omega_m \approx \omega_o)$ within a cavity resonance peak. This results in red-shift and blue-shift of a $|\phi_{max}|$, with respect to a resonance amplitude peak, for the upward and downward frequency scans, respectively.

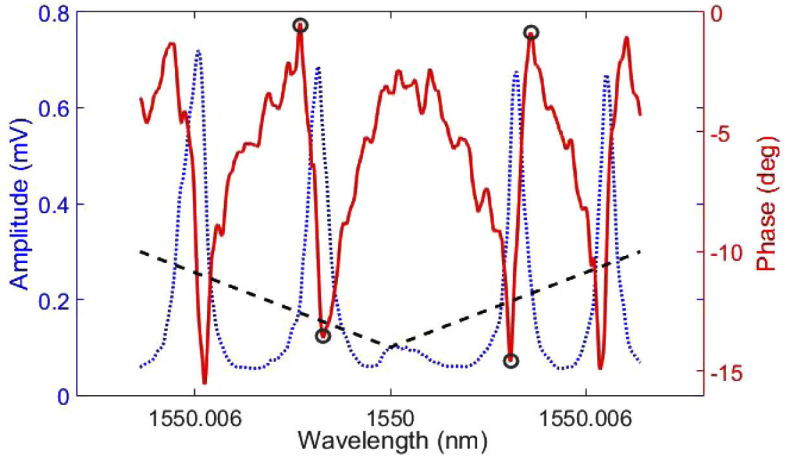


Fig. 4. Representative CAPS data. The black dashed curve represents a part of the triangular wave used for the wavelength modulation. The left and right hand sides of the 1550 nm point show downward and upward wavelength scans, respectively. The blue dotted curve shows resonance peaks. The red solid curve shows phase measurements using our wavelength scanned CAPS technique.

The AFM1 solution, derived from the aspergillus flavus, is purchased from Sigma-Aldrich Inc. USA. We then dilute it in DI water for preparing its various concentrations. We start our measurements with DI water, followed by a known AFM1 concentration solution. We use the assumption of reaching a steady state after injecting an AFM1 solution. We wait for one to two minutes after the injection of a sample for conducting a CAPS measurement. In our measurements, we inject an AFM1 solution right in the vicinity of the taper into the fluidic cell by using a standard syringe, as shown in Fig. 3. We see a change in phase on the lock-in amplifier within a few seconds of the injection. This phase change then stays constant. The AFM1 binding on the functionalized fiber is so strong that after recording CAPS measurements with each AFM1 sample, we rinse the fluidic cell along with the tapered fiber first with a glycerine based buffer solution and then afterward with DI water. This rinsing step removes any AFM1 binding event, and consequently, the functionalized tapered fiber is recycled for a new measurement. A strong binding also indicates that the steady state reaches quickly, as also shown in Ref. [10].

The phase shift data collected from the lock-in amplifier is analyzed in MATLAB. For our experimental conditions, we approximately see around nineteen peaks in an upward or

Optics EXPRESS

downward wavelength scan. We subtract the maximum and minimum phase of each phase peak (representative data shown by circles in Fig. 4) in one scan and then take the mean of all the differences, which gives one phase measurement, ϕ, for an injected sample. The measured phase, ϕ, due to CAPS for various concentrations of AFM1 solutions is shown in Fig. 5(a). We also see that cotangent(ϕ) is proportional to AFM1 concentrations. This trend is consistent with Eq. (3) as the ring down time is inversely proportional to the AFM1 concentration.

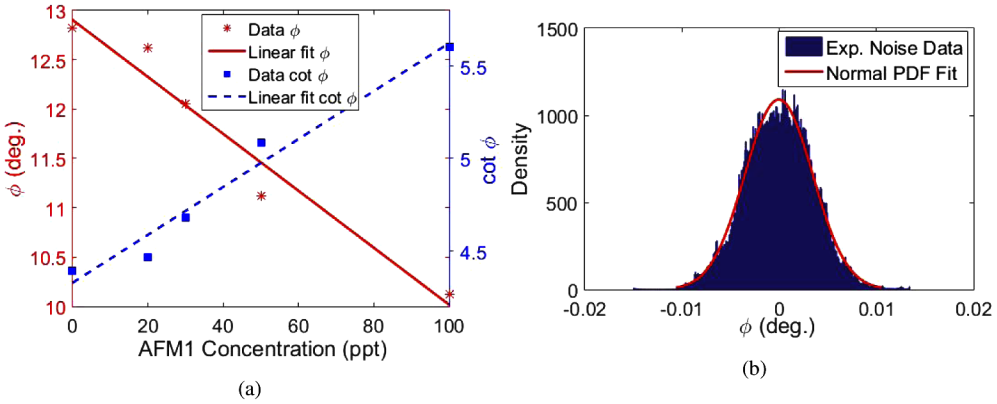


Fig. 5. (a) Experimental results for detecting AFM1 using CAPS. (b) Noise data of the CAPS sensing setup

From these results, we can see that our demonstrated CAPS sensor has the sensitivity and detection limit of 0.029^o/ppt and 20 ppt, respectively (1 ppt=1 ng/L). The sensor's noise is measured by taking the laser out of the cavity resonance by changing its temperature so that its wavelength peak is out of the reflection spectrum of the two FBGs. We then continuously monitor the phase data coming from the sensor. In this way, the laser beam has a contribution from all components present in the sensing setup, including the function generator, modulator, polarization controller, SMF-28 fibers, detector, and lock-in amplifier (See Fig. 3). The baseline phase and its variations due to noise of all components are thus captured. We also keep all instruments on and with the same settings during the noise measurements as in AFM1 measurements. The noise histogram data, along with the normal probability distribution fit, is shown in Fig. 5(b). The fit shows that one standard deviation, i.e., noise is 0.003 °.

The concentration in an unknown sample can be estimated from the response curve accordingly to the phase observed for it. We also see that as the AFM1 concentration increases, the phase decreases. This trend is due to the increase in the cavity losses caused by the AFM1 binding events. We also try to measure similar AFM1 concentrations with a non-functionalized tapered fiber and find no phase changes. This indicates that functionalizing the sensing head is critical for detecting lower concentrations. We also note that at 1550 nm, there will be a background absorption in aqueous solutions. We can minimize the impact of this attenuation by using an amplifier inside the cavity, i.e., one can employ amplified CAPS measurements as reported in [24] recently. Since we are meeting the required detection limits in the current work, the amplifier is not included to keep the overall setup less complicated.

4. Conclusion

In this work, we demonstrate the first application of CAPS to fiber cavities for detecting AFM1 in a solution. The experimental results obtained depict AFM1 detection as low as 20 ng/L, which is well below the safety limits laid down by both the US and the European regulatory authorities. Compared to traditional and previous AFM1 sensors, the demonstrated sensor

Optics EXPRESS

modality offers a reduction in detection time and cost, minimum sample pre-treatment, decrease in system complexity, lower fabrication challenges, and increased potential for portability. There are various future directions for improving the present work. These include testing with actual milk samples, introducing temperature-controlled environments for the FBGs and fluidic cell, and improving and optimizing parameters for tapering fibers to enhance sensor sensitivity. We anticipate that the demonstrated sensing setup with alteration to the surface chemistry protocol will lead to an inexpensive, realtime, and a reliable optical sensor for numerous applications in food security, health, environmental, and agricultural sectors, especially in low-resource settings.

Funding. Pakistan Science Foundation (PSF-TUBITAK/P-LUMS (3)).

Acknowledgment. We would like to thank Hazem Asif for helping us in drawing Fig. 3 of the experimental schematics.

Disclosures. The authors declare no conflicts of interest.

References

1. E. E. Creppy, "Update of survey, regulation and toxic effects of mycotoxins in europe," Toxicol. Lett. **127**(1-3), 19–28 (2002).
2. F. Joint, W. H. Organization, and W. E. C. on Food Additives, *Evaluation of certain contaminants in food: eighty-third report of the Joint FAO/WHO Expert Committee on Food Additives* (World Health Organization, 2017).
3. H. Yao, Z. Hruska, and J. D. Di Mavungu, "Developments in detection and determination of aflatoxins," World Mycotoxin Journal **8**(2), 181–191 (2015).
4. Y. Wang, J. Dostálek, and W. Knoll, "Long range surface plasmon-enhanced fluorescence spectroscopy for the detection of aflatoxin m1 in milk," Biosens. Bioelectron. **24**(7), 2264–2267 (2009).
5. C. Cucci, A. Mignani, C. Dall'Asta, R. Pela, and A. Dossena, "A portable fluorometer for the rapid screening of m1 aflatoxin," Sens. Actuators, B **126**(2), 467–472 (2007).
6. M. Mahfuz, M. A. Gazi, M. Hossain, M. R. Islam, S. M. Fahim, and T. Ahmed, "General and advanced methods for the detection and measurement of aflatoxins and aflatoxin metabolites: a review," Toxin Rev. **39**(2), 123–137 (2020).
7. X. D. Hoa, A. Kirk, and M. Tabrizian, "Towards integrated and sensitive surface plasmon resonance biosensors: a review of recent progress," Biosens. Bioelectron. **23**(2), 151–160 (2007).
8. R. Guider, D. Gandolfi, T. Chalyan, L. Pasquardini, A. Samusenko, G. Pucker, C. Pederzolli, and L. Pavesi, "Design and optimization of sion ring resonator-based biosensors for aflatoxin m1 detection," Sensors **15**(7), 17300–17312 (2015).
9. M. I. Cheema, S. Mehrabani, A. A. Hayat, Y.-A. Peter, A. M. Armani, and A. G. Kirk, "Simultaneous measurement of quality factor and wavelength shift by phase shift microcavity ring down spectroscopy," Opt. Express **20**(8), 9090–9098 (2012).
10. T. Chalyan, C. Potrich, E. Schreuder, F. Falke, L. Pasquardini, C. Pederzolli, R. Heideman, and L. Pavesi, "Afm1 detection in milk by fab'functionalized si3n4 asymmetric mach–zehnder interferometric biosensors," Toxins **11**(7), 409 (2019).
11. J. M. Herbelin and J. A. McKay, "Development of laser mirrors of very high reflectivity using the cavity-attenuated phase-shift method," Appl. Opt. **20**(19), 3341–3344 (1981).
12. J. Scherer, J. Paul, A. O'keefe, and R. Saykally, "Cavity ringdown laser absorption spectroscopy: history, development, and application to pulsed molecular beams," Chem. Rev. **97**(1), 25–52 (1997).
13. G. Berden, R. Peeters, and G. Meijer, "Cavity ring-down spectroscopy: Experimental schemes and applications," Int. Rev. Phys. Chem. **19**(4), 565–607 (2000).
14. R. Engeln, G. von Helden, G. Berden, and G. Meijer, "Phase shift cavity ring down absorption spectroscopy," Chem. Phys. Lett. **262**(1-2), 105–109 (1996).
15. P. L. Kebabian, S. C. Herndon, and A. Freedman, "Detection of nitrogen dioxide by cavity attenuated phase shift spectroscopy," Anal. Chem. **77**(2), 724–728 (2005).
16. C. Vallance and C. M. Rushworth, "Cavity ringdown spectroscopy for the analysis of small liquid volumes," in *Cavity-Enhanced Spectroscopy and Sensing*, (Springer, 2014), pp. 385–410.
17. J. E. Thompson, "Cavity-enhanced spectroscopy in condensed phases: Recent literature and remaining challenges," Journal of Spectroscopy **2017**, 1–10 (2017).
18. J. A. Barnes, G. Gagliardi, and H.-P. Loock, "Phase-shift cavity ring-down spectroscopy on a microsphere resonator by rayleigh backscattering," Phys. Rev. A **87**(5), 053843 (2013).
19. Z. Tong, A. Wright, T. McCormick, R. Li, R. D. Oleschuk, and H.-P. Loock, "Phase-shift fiber-loop ring-down spectroscopy," Anal. Chem. **76**(22), 6594–6599 (2004).
20. W. Chen, C. Zhao, B. Mao, H. Chen, and C. Shen, "Detection of aflatoxin b 1 in food based on smf taper combined with fiber loop ring down technique," IEEE Sens. J. **20**(5), 2446–2451 (2019).
21. R. Guider, D. Gandolfi, T. Chalyan, L. Pasquardini, A. Samusenko, C. Pederzolli, G. Pucker, and L. Pavesi, "Sensitivity and limit of detection of biosensors based on ring resonators," Sensing and bio-sensing research **6**, 99–102 (2015).
22. H. A. Haus, *Waves and fields in optoelectronics* (Prentice-Hall, 1984).

Optics EXPRESS

23. M. I. Cheema and A. G. Kirk, "Analytical expressions for waveguide-coupled phase shift microcavity ring down spectroscopy," J. Opt. Soc. Am. B **32**(2), 355–362 (2015).
24. M. I. Cheema, U. Ullah, M. D. Ghauri, R. A. Ayaz, Y. Uysalli, B. Morova, and A. Kiraz, "Amplified phase shift–fiber cavity ring down spectroscopy for biosensing applications at 1550nm," in *Frontiers in Biological Detection: From Nanosensors to Systems XII*, vol. 11258 (International Society for Optics and Photonics, 2020), p. 112580G.